Int. J. Electrochem. Sci., 15 **(2020)** 1771 – 1787, doi: 10.20964/2020.02.35

International Journal of
ELECTROCHEMICAL
SCIENCE
www.electrochemsci.org

Detection of Hydrochlorothiazide, Sulfamethoxazole, and Trimethoprim at Metal Oxide Modified Glassy Carbon Electrodes

Mohammad F. Khanfar[1,], Eyad S. M. Abu-Nameh[2,*], Munib M. Saket[1], Lujain T. Al Khateeb[1], Akram Al Ahmad[2], Zeinab Asaad[1], Zaina Salem[1], and Nasim Alnuman[3]*

[1] Pharmaceutical-Chemical Engineering Department, School of Applied Medical Sciences, German Jordanian University, P.O.Box 35247 Amman 11180 Jordan
[2] Department of Chemistry, Faculty of Science, Al-Balqa Applied University, Al-Salt 19117, Jordan
[3] Biomedical Engineering Department, School of Applied Medical Sciences, German Jordanian University, P.O.Box 35247 Amman 11180 Jordan
[*]E-mail: mohammad.khanfar@gju.edu.jo (M. F. Khanfar); abunameh@bau.edu.jo (E. S. M. Abu-Nameh)

Received: 29 March 2019 / *Accepted:* 5 August 2019 / *Published:* 31 December 2019

Molybdenum and manganese oxides are well-known electro-catalysts in fuel cells systems, they are usually used as anodic materials for the oxidation of low molecular weight alcohols. The utilization of MoO_2 and MnO_2 as catalysts in the pharmaceutical analysis is not common yet. In this study, bare glassy carbon electrodes were modified by the oxides by means of electrochemical deposition and the modified electrodes were used as catalysts for the electrochemical oxidation of sulfamethoxazole (SMX), trimethoprim (TMP), and hydrochlorothiazide (HCT). Well-resolved anodic peaks were reported for the analyzed pharmaceuticals when the MoO_2/GCE was used for the simultaneous analysis of the SMX and TMP and when MnO_2/GCE was utilized for the analysis of HCT. Analytical performance of the modified electrodes was evaluated based on the following statistical parameters; linearity ranges, correlation coefficients, limits of detection and quantitation, and recovery values. The prepared electrodes were used for the determination of the active ingredients in their pharmaceutical formulations and the reported activity was correlated to influence of the utilized pH on both structures of the used electrodes and the detected analytes.

Keywords: Molybdenum (IV) oxide, manganese (IV) oxide, sulfamethoxazole, trimethoprim, hydrochlorothiazide

1. INTRODUCTION

In the 16th century, the role of diuretics began when they were solely introduced to remove fluid accumulation in the body for the treatment of edema [1-3]. Later, in 1957, Sharp and Dohme (now

Merck) modernized the concept of diuretic therapy by the introduction of thiazides, as anti-hypertensive agents, which proved to lower blood pressure as a secondary consequence [4].

A prototypic member, Hydrochlorothiazide (HCT), was first sold commercially in early 1959 and still remains to be the most widely prescribed drug of thiazide class for the treatment of hypertension and edema [5]. This is because HCT has a half-life of 8-12 hours which permits effective once-daily doses in comparison with all other thiazide diuretics. HCT is only administered orally in three doses: 12.5, 25, and 50 mg tablets. Following oral administration, the drug is well absorbed (65-75%) and 55%-77% of the administered dose appears in the urine. In addition, more than 95% of the absorbed dose is excreted in urine as an unchanged drug (i.e. not metabolized) within 24 hours [6-8].

HCT is chemically designated as 6-Chloro-3,4-dihydro-2H-1,2,4-benzothiadiazine-7-sulfonamide 1,1-dioxide with five main functional groups: an aromatic ring, halide group, secondary amino group, cyclic and acyclic sulfonamide groups. Industrially, the drug is synthesized by either the reaction of para-formaldehyde with 5-chloro-2,4-disulfamoylaniline in nonaqueous media or the reaction of formaldehyde with 6-chloro-7-sulfamoyl-2H-1,2,4-benzothiadiazine-1,1-dioxide in an aqueous alkaline solution of ammonia [9].

SMX and TMP are abbreviations for Sulfamethoxazole and Trimethoprim. They are antibacterial agents that are used to treat bacterial infections. SMX and TMP pharmaceutical formulation is an important progress in the development of antimicrobial agents (antibiotics). This combination increases the sulfa bacteriostatic effect and since 1969, SMX has been used mainly in combination with TMP at a fixed ratio of 5:1 [10]. Those products are usually mixed with other drugs to increase their efficiency. Sulfamethoxazole (SMX) is N-(5-methyl-3-isoxazolyl) sulfanilamide, which belongs to the family of sulfonamides; SMX interferes with folic acid synthesis in sensitive bacteria. SMX and other sulfonamides act as competitive inhibitors of the enzyme dihydropteroate synthase, an enzyme involved in folate synthesis. Therefore, sulfonamides are considered as bacteriostatic; they inhibit the growth of bacteria but do not kill them. SMX is one of the most active pharmaceutical ingredients of the antibiotics that are usually used in the treatment of urinary tract infection, chronic bronchitis, and meningococcal meningitis. Trimethoprim (TMP), which is a synthetic derivative of trimethoxybenzyle-pyrmidine with anti-bacterial and anti-protozoal properties. Trimethoprim binds to the bacterial enzyme dihydrofolate reductase in which it blocks the production of tetrahydrofolic acid. [11]. Chemical structures of SMX, TMP, and HCT are shown in Fig. 1.

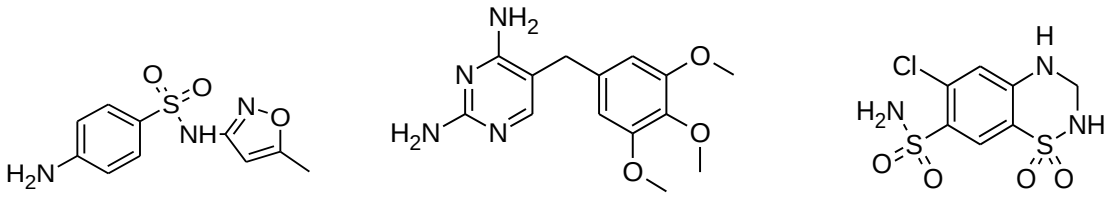

Figure 1. Chemical structures (from left to right) of sulfamethoxazole, trimethoprim, and hydrochlorothiazide

Due to the increasing frequency at which SMX, TMP, and HCT are prescribed, there is a continuous demand to develop new analytical techniques for their accurate determination. In a vast

number of pharmaceutical industries, especially in Jordan, almost all of the attention is paid to chromatographic and photometric methods which are not cost effective, require well-trained operators, and time-consuming. [12-23] Voltammetric analysis is quick and simple, therefore, the utilization of voltammetry as a tool for the assay of active pharmaceutical ingredients should be encouraged. However, the majority of modified electrodes developed for voltammetric studies require complex preparation. [24-44] In view of these challenges, the prepared electrodes in this study provide a promising platform for the construction of easy to use, rapid, and cost-effective analytical tool for detection of the three pharmaceuticals. Sulfamethoxazole, trimethoprim, and hydrochlorothizide do share one electrochemical property in common, they all undergo irreversible oxidation reactions as shown in Fig. 2. The generated oxidation current is directly proportional to the oxidized species concentration and that's how a calibration curve, that correlates the pharmaceutical oxidation current to its corresponding concentration, is constructed. As shown in Fig. 2, SMX and TMP are oxidized to their corresponding iminobenzoquinone and nitroso counterparts, respectively, while HCT is oxidized to its imine analog.

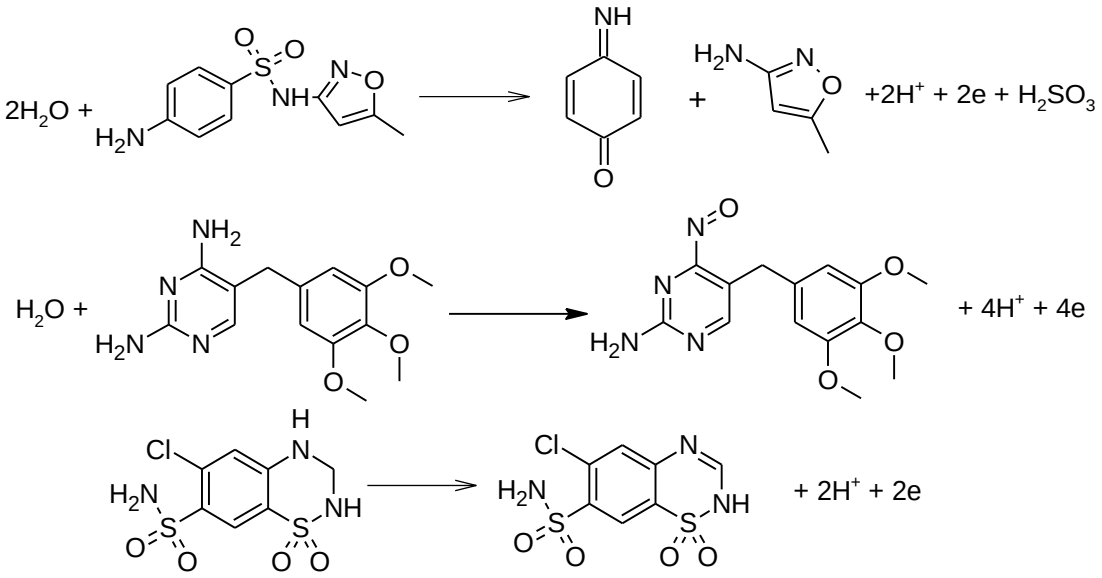

Figure 2. Electrochemical oxidation reactions (from top to bottom) of sulfamethoxazole, trimethoprim, and hydrochlorothiazide

The utilization of manganese and molybdenum oxides as oxidizing agents in pharmaceutical electroanalysis is not common. These oxides have electron deficient metallic centers of high oxidation states, therefore, carbon-based electrodes modified with these oxides have the potential to oxidize a wide range of organic compounds such as alcohols and alkanes more efficiently than their bare counterparts. Molybdenum modified electrodes are usually used for promotion of methanol and ethanol oxidation in fuel cells systems where the alcohol adsorption and the following oxidation is enhanced in the presence of molybdenum. Molybdenum is utilized as co-catalyst besides the key fuel cells catalysts such as platinum, platinum-based alloys, and complexes with platinum as the metallic center. [45-48] There are few examples in the literature on the utilization of manganese oxide for the oxidation of pharmaceuticals. Ascorbic acid, riboflavin, and indomethacin have been detected by carbon-based electrodes modified

with manganese dioxide. [49-51] Role of the mentioned metallic oxides as either oxidizing agents, catalysts, or both still needs further investigation. In this work, glassy carbon electrodes were modified with molybdenum and manganese oxides by means of electrochemical deposition and the modified electrodes were used for HCT, SMX, and TMP determination in locally provided pharmaceutical dosage forms. Details of the modification and the assay will be demonstrated within the context of the following sections.

2. EXPERIMENTAL

2.1 Chemicals and Solutions

Sulfamethoxazole, trimethoprim, and hydrochlrothizide were provided by Sigma-Aldrich Chemie GmbH, Darmstadt, Germany. Sodium hydroxide, potassium chloride, boric acid, and phosphoric acid were all provided by VWR chemicals, NY, U.S.A. Glacial acetic acid, sodium molybdate, sodium sulfate, and potassium permanganate were purchased from S D Fine-Chem Ltd., Mumbai, India. The commercial products (Brand A, Brand B, Brand C, and Brand D) were purchased from the local market.

The measurements were carried out using Britton-Robinson pH = 7.00 for SMX and TMP analysis or pH = 3.00 for HCT analysis. To prepare the buffer solutions, the appropriate amounts of phosphoric, boric, and glacial acetic acids were dissolved in ultrapure water (Ultra Max 372, Yong Lin Instrument Co., Ltd, Anyang, Korea). pH of the buffer solutions was adjusted by the addition of the required amount of 0.100 M NaOH. The pH values were determined by SevenGo Duo pH meter supplied by Mettler-Toledo, AG, Analytical, Schwerzenbach, Switzerland.1.00 mM of potassium permanganate and 10.0 mM of potassium chloride solution was prepared and used for MnO_2 deposition. For the deposition of MoO_2, an aqueous solution of 1.00 mM of sodium molybdate and 10.0 mM of sodium sulfate was prepared, then used.

2.2 Instruments and Measurements

All of the voltammetric experiments were performed in three compartment glass cell using Ag/AgCl and platinum as the reference and the counter electrodes, respectively. The glassy carbon working electrode (3.0 mm i.d.) and the rotator used were provided by Pine Research Instrumentation, NC, U.S.A. PGSTAT101 Autolab potentiostat (Metrohm, Utrecht, The Netherlands) operated by NOVA 2.2 and connected to a personal computer was used to perform the electrochemical experiments. For scanning electron microscopic imaging, VEGA3 scanning electron microscope (Tescan, Brno, Czech Republic) was used.

2.3 Electrode Fabrication

The glassy carbon electrodes were polished, then rinsed with distilled water, and dried. For deposition of the manganese oxide, potential of the carbon electrode was cycled between 0.20 and -0.80

V at 25 mV/s for six cycles. The electrode was then removed from the deposition cell, rinsed with distilled water and left to dry. Deposition of Mo (IV) oxide was performed by cycling potential of the glassy carbon electrode at 10 mV/s between 0.60 and -0.10 V for two cycles, then the electrode was removed from the cell, rinsed with distilled water and left to dry. The prepared electrodes will be referred to in the following sections as MnO_2/GCE and MoO_2/GCE. After the described modification was performed, the modified electrodes were imaged and used for the HCT, SMX, and TMP voltammetric detection.

2.4 Analytical Procedure

For preparation of the standard solutions, 5.00 mM stock Britton-Robinson buffer solutions were prepared. Standard solutions of SMX, TMP, and HCT were then prepared from the stock by serial dilution. The prepared series was employed for establishing the calibration curve that correlates the oxidation peak current to the corresponding analyte concentration.

The voltammetric measurements were performed using the differential pulse voltammetric (DPV) mode with the following parameters;

Potential Step	0.005 V
Modulation amplitude	0.025 V
Modulation time	0.05 s
Interval time	0.5 s
Scan rate	0.01007 V/s

Unless otherwise stated, all of the voltammetric measurements were performed in the hydrodynamic mode with rotation speed equals to 50 rpm. To establish the calibration curve, potential of the modified electrode was scanned between 0.00 and 1.25 V versus Ag/AgCl for SMX/TMP analysis or 0.00 and 1.40 V for HCT detection. The oxidation peak current obtained from each measurement was plotted versus the corresponding solution concentration.

2.5 Samples Preparation

To obtain percentage recovery of the pharmaceuticals in the commercial drugs using the modified GCEs, one tablet of each of the three provided drugs was weighed and powdered with mortar and pestle. The powder was then accurately transferred to 100 ml volumetric flask and diluted to the mark with the prepared buffer solutions. The solution was then sonicated for 10 minutes, filtered, and a fraction of the filtrate was pipetted and used for the recovery evaluation.

% recovery was then estimated based on the following equation;

$$\% \text{ recovery} = ([(S_{x+s}) - S_x]/S_s) \times 100\%$$

Where S_x and S_s are the oxidation peak current values for the sample and the standard pharmaceutical solutions, respectively, and S_{x+s} is the oxidation peak current for mixtures of equal volumes of the standard and the sample solutions.

3. RESULTS AND DISCUSSION

3.1. Deposition of the metal oxides

The deposition of molybdenum and manganese oxides was performed successfully in this work, as shown in Fig. 3. Surface of the unmodified electrode is shown in Fig. 3-A, scratches in the carbon surface were originated from the mechanical polishing of the bare electrode surface among the voltammetric measurements. Molybdenum oxide was deposited in the form of needle-like aggregates scattered over the carbon surface, as presented in Fig. 3-B. Electrochemically, the deposition occurs according to;[52]

$$MoO_4^{2-} + 4H^+ + 2e \rightarrow MoO_2 + 2H_2O$$

Manganese dioxide was electro-deposited on the glassy carbon surface in the form of a thick film, as shown in Fig. 3-C. The deposition process could take place according to; [53]

$$MnO_4^{2-} + 4H^+ + 2e \rightarrow MnO_2 + 2H_2O$$

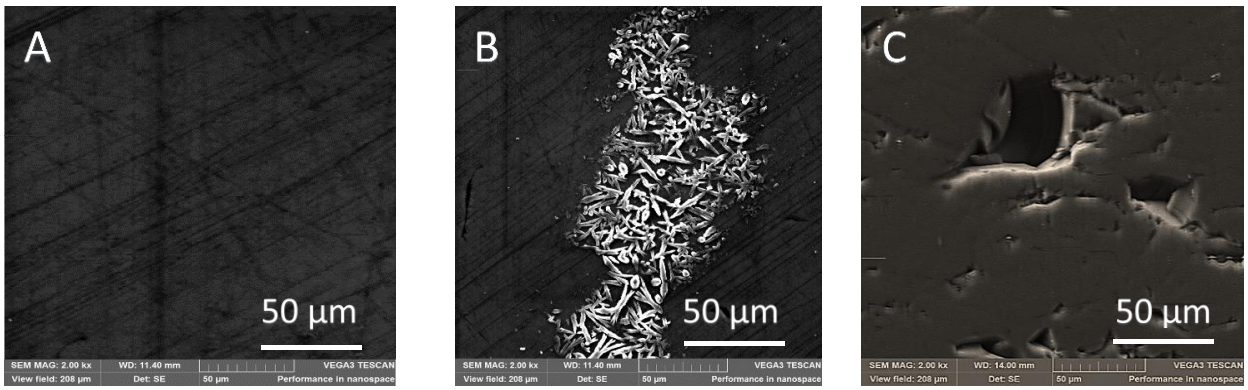

Figure 3. SEM images of (A) bare, (B) molybdenum modified, and (C) manganese modified glassy carbon electrodes

Features of the deposited oxides depend on different factors such as the initial salt concentration, nature of the template, the utilized pH value, the applied electrochemical signal, and the presence of other ions that may undergo electrolysis, along with the target species. Therefore, the deposited oxides do not follow any pattern in specific, and each pattern has its own features, physical, and chemical properties.

3.2. Oxidation of the target pharmaceuticals

Both of MnO_2 and MoO_2 have been examined as catalysts for the oxidation of the three drugs under investigation. The manganese oxide exhibited a significant activity toward the oxidation of hydrochlorothiazide while molybdenum oxide has been found active toward the oxidation of sulfamethoxazole and trimethoprim. Two well-defined oxidation peaks are shown in Fig. 4, at 880 and 1130 mV versus Ag/AgCl. The two peaks could be attributed to the oxidation of SMX and TMP, respectively. Fig. 4 also shows the higher catalytic activity of the modified surface, over its bare

counterpart, which could be attributed to two factors, increase of the electron transfer rate across the solution-electrode interface in presence of the oxide, and the catalytic role of the modifier, the molybdenum oxide, which will be discussed in section 3.4.

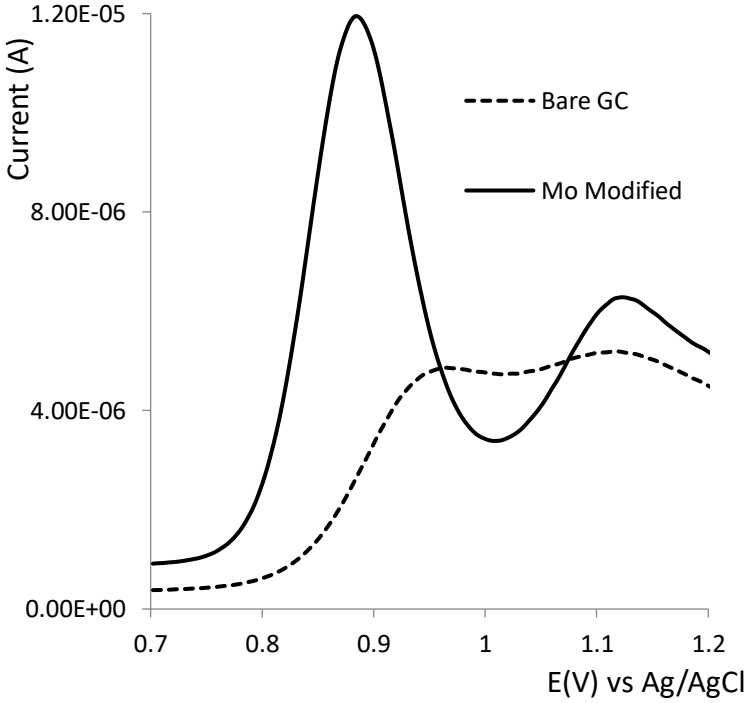

Figure 4. Differential pulse voltammograms of the bare and the molybdenum modified glassy carbon electrode in pH 7.00 BR buffer solution containing 2.0mM SMX and 10.0mM TMP

Effect of the employed pH on the oxidation of the SMX and TMP is demonstrated in Fig. 5. The figure shows the DPV of the modified surface at three different pH values. The presence of two well-resolved peaks was reported in neutral media at pH 7.00, the utilization of higher pH values is accompanied by attenuation of the oxidation peaks, as it is the case at pH 9.00. As will be illustrated in the coming section, selection of the desired pH value is based on the presence of both of the target analyte and the catalyst in the forms that secure optimum detection conditions.

The oxidation of HCT at the manganese-modified electrode is presented in Fig. 6. The oxidation current at the modified surface is three times higher than that reported at the bare electrode. The conductive nature of the added modifier is one of the two factors behind the reported activity. The other factor is the role of the manganese oxide as both oxidizing agent and catalyst. Voltammograms of the manganese-modified electrode in HCT buffered solutions are presented in Fig. 7. The highest catalytic activity was reported at pH 3.00, the highest oxidation peak is shown at 1183 mV and the height of the peak decreases as the pH increases. At pH 12.2 the peak has disappeared entirely. The correlation between the utilized pH, activity of the catalyst, and structure of the analyzed species will be discussed in section 3.4.

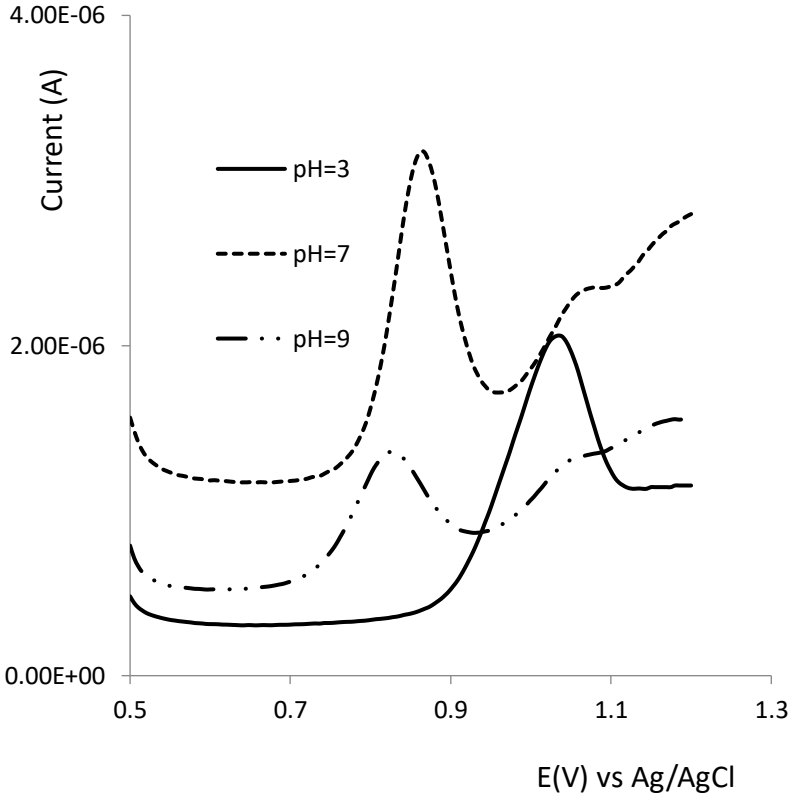

Figure 5. Differential pulse voltammograms of the molybdenum modified glassy carbon electrode in pH 3.00, 7.00, and 9.00 BR buffer solutions containing 10.0mM SMX and 2.0mM TMP

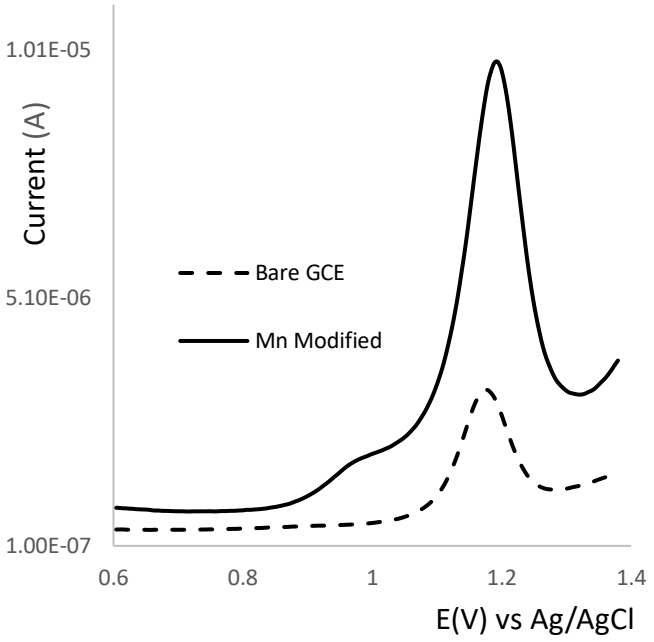

Figure 6. Differential pulse voltammograms of the bare and the manganese-modified glassy carbon electrode in pH 3.00 BR buffer solution containing 2.0mM HCT

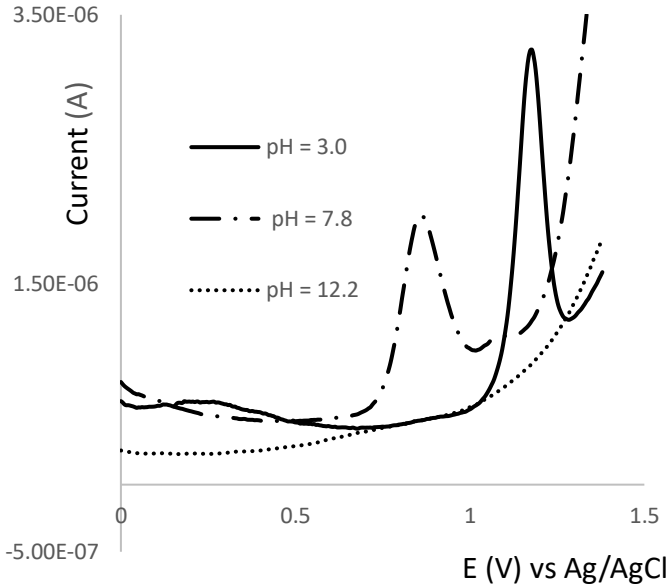

Figure 7. Differential pulse voltammograms of the manganese modified glassy carbon electrode in pH 3.00, 7.80, and 12.2 BR buffer solutions containing 2.0mM HCT

3.3. Statistical Evaluation of Performance of the Modified Electrodes

In this work, the dependence of the oxidation peak current on rate of the scanned potential was investigated for the three analyzed species. With all of the studied pharmaceuticals, it was found that the oxidation current, as studied by linear scan voltammetry (LSV), is dependent on square root of the scan rate (Fig. 8). Therefore, all of the oxidation processes are diffusion, rather than surface, controlled faradaic processes and the produced current originates from diffusion of the active species from the bulk of the solution to the modified electrode surface, where the predicted oxidation processes take place.

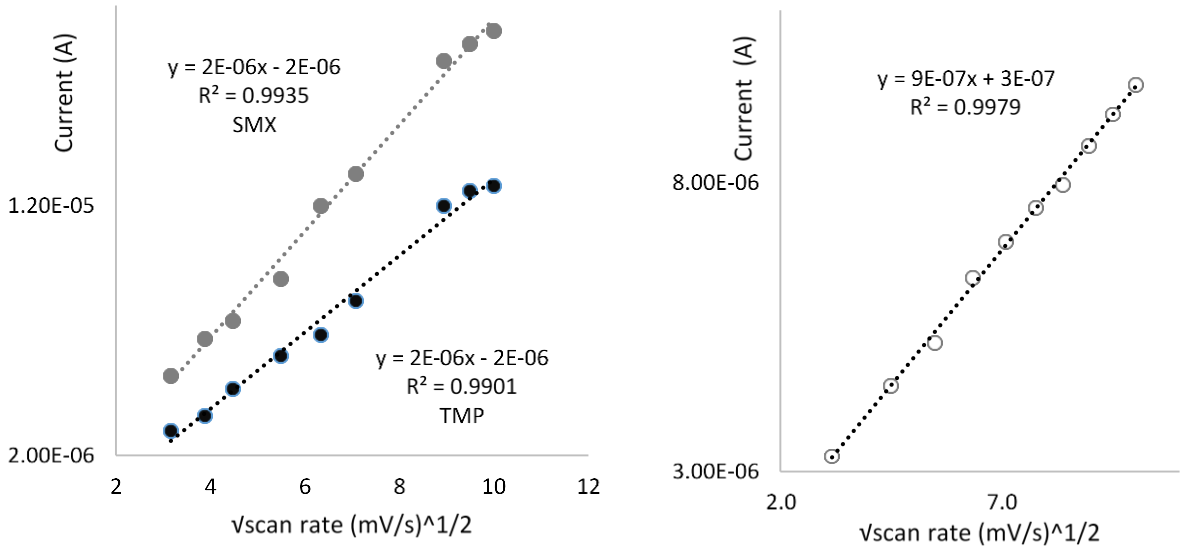

Figure 8. Dependence of the oxidation peak current on square root of the scan rate

The reported activity of the manganese and molybdenum oxides was examined in a systematic approach. Calibration curves that correlate the oxidation peak current values to concentrations of the target analytes were established based on the corresponding differential pulse voltammetric measurements. Dependence of the SMX, TMP, and HCT peak current values on the corresponding drugs concentrations are presented in Figs. 9 and 10.

In this context, it is worth to mention that there are cases where the peak current values are not in a linear relationship with their corresponding concentrations, for example, when working electrodes are modified with relatively thick layers of modifiers. In such cases, while running LSV or DPV experiments, the current values observed at beginning of the scan are much higher than the corresponding values reported when the corresponding bare -unmodified- electrodes are used, because of the presence of the added modifiers. As a consequence, the voltammogram may need a background correction since all of the current values will be shifted to higher values if the oxidation reaction is taking place for example. Therefore, one could count on peak areas to construct the correlation between charge and concentration, and determine the statistical parameter based on the established correlation. [54]

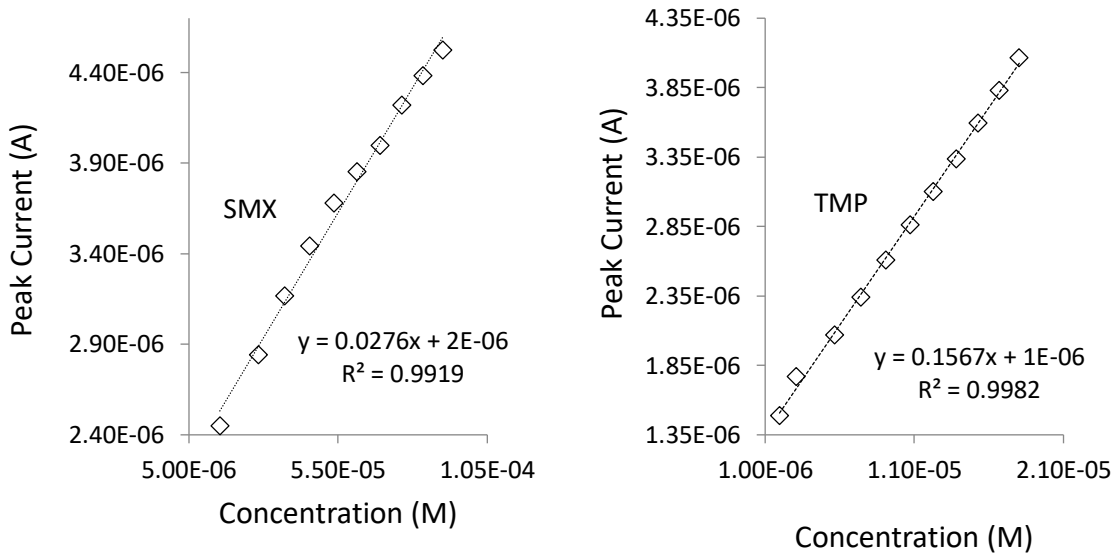

Figure 9. Dependence of oxidation peak current on SMX and TMP concentration, detected in pH 7.00 BR buffer solution

All of the obtained statistical parameters are listed in table 1. As shown in the table, the molybdenum modified electrode exhibits higher sensitivity toward SMX and TMP detection, when compared to the manganese-modified electrode utilized for the detection of HCT. That variation could be attributed to the nature of the deposited layer, since manganese is less conductive than the molybdenum.

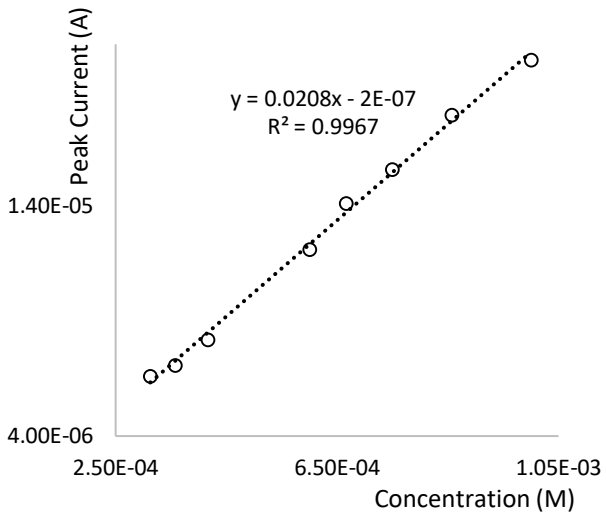

Figure 10. Dependence of HCT oxidation peak current on HCT concentration, detected in pH 3.00 BR buffer solution

Table 1. Statistical parameters for the oxidation of SMX, TMP, and HCT at the modified surfaces (*N=5*)

Analyte	Catalyst	R^2	Linear Range (µM)	L.O.D. (µM)	L.O.Q. (µM)
SMX	MoO_2	0.992	10.0-100.	0.144	0.432
TMP	MoO_2	0.998	2.00-20.0	0.127	0.381
HCT	MnO_2	0.997	$3.00x10^2$-$1.00x10^3$	5.86	17.9

Performance of the modified electrodes was compared to those prepared by other research groups as shown in tables 2 and 3. The catalytic activity of the manganese oxide electrode used for the detection of HCT is less than that of the different carbon-based electrodes, as shown in table 2. Most of the listed electrodes have activity higher than that reported for the manganese oxide electrode prepared in this study. Improvement of performance of the modified electrode could be achieved by doping of the manganese layer with conductive ingredients such as carbon black, carbon fibers, or carbon nanotubes, which have high surface areas and therefore, enhance the utilization of manganese oxide as both catalyst and oxidizing agent. As a consequence, the electrode is expected to demonstrate a higher sensitivity toward HCT detection. Besides doping; thickness of the manganese oxide layer could be varied and correlated to the oxide catalytic activity.

Table 2. Comparison of activity of MnO_2/GCE with other modified electrodes for HCT determination

Electrode	Technique	Linear Range (µM)	LOD (µM)	Reference
H-GRE	DPV	0.10-48	$1.9x10^{-2}$	[32]
Melamine/ Fe_3O_4	SWV	0.025-10.	$4.0x10^{-3}$	[33]
BDDE	DPV	3.0-74	1.2	[34]
NiOH/Ni	CV	13.9-167	7.92	[35]
SPCE/PGA	DPV	28.5–300.	8.55	[36]
SPCE/EGA		3.78–200.	1.13	
MnO_2/GCE	DPV	$3.00x10^2$ – $1.00x10^3$	5.86	This work

As shown in table 3, the molybdenum oxide modified electrode exhibits an activity that is comparable with the activity of the other electrodes. Only multi-walled carbon nanotube modified electrodes have better performance toward detection of the two antibiotics, that could be attributed to the high dispersion of the employed catalyst, the antimony nanoparticles over the high surface area carbon tubes, that configuration secures the presence of huge number of catalytic sites available for the simultaneous oxidation of SMX and TMP.

Table 3. Comparison of activity of MoO_2/GCE with other modified electrodes for SMX/TMP detection

Electrode	Technique	Linear Range (µM)	LOD (µM)	Reference
MWCNT-SbNPs	DPV	0.10–0.70	$24x10^{-3}$ (SMX) $31x10^{-3}$ (TMP)	[40]
MWCNT/PBnc/SPE	DPV	1.0–10. (SMX) 0.10–10. (TMP)	$38x10^{-3}$ (SMX) $60x10^{-3}$ (TMP)	[41]
GC/rGO-AgNP	DPV	1.0-10.	0.60 (SMX) 0.40 (TMP)	[42]
HT-BDD	DPV	1.00-10.0 ppm (SMX) 0.200-2.00 ppm (TMP)	3.65 (SMX) 3.92 (TMP)	[43]
GCE	SWV	55.0- 395 (SMX) 10.5-104 (TMP)	8.52 (SMX) 0.931 (TMP)	[44]
MoO_2/GCE	DPV	10.0-100. (SMX) 2.00-20.0 (TMP)	0.144 (SMX) 0.127 (TMP)	This work

Recovery of the pharmaceuticals in their dosage forms was also studied in this work, as described in section 2.5. Fixed volumes of the target analytes were spiked with different volumes of the corresponding standard solutions. One of the trials performed for estimation of the HCT recovery, presented as an example, is shown in Fig. 11. As shown in the figure, spiking does not have any significant impact on position of the peak potential, variation in the position of the peak voltage is less than 20 mV. All of the recovery values are listed in table 4. All of the values listed in the table are within the acceptable range between 80 and 120 %.

Table 4. Recovery percentages of the active ingredients in their pharmaceutical forms (*N=3*)

Brand	Active Ingredients	Declared Content (mg per tablet)	Catalyst	% Recovery
Brand A	HCT	50	MnO_2	110%
Brand B		25		108%
Brand C	SMX	400	MoO_2	94.4%
	TMP	80		89.6%
Brand D	SMX	400		111%
	TMP	80		96.7%

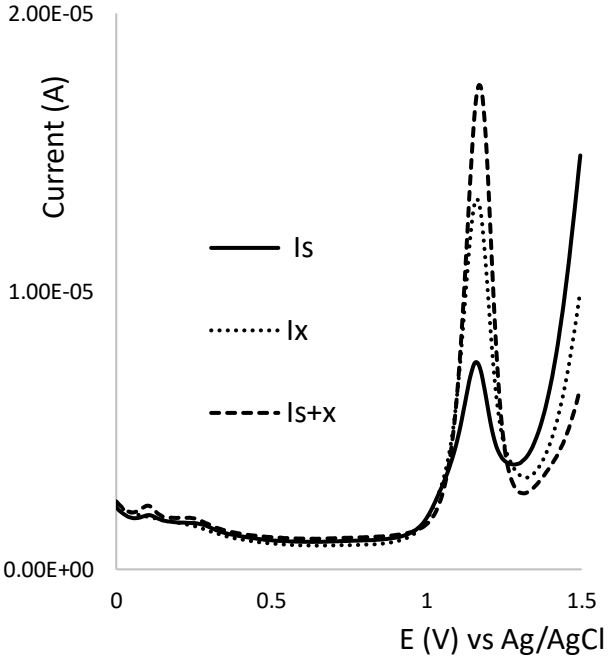

Figure 11. Differential pulse voltammograms of the manganese-modified glassy carbon electrode in pH 3.00 BR buffer solutions containing standard HCT (Is), unknown HCT (Ix), and a mixture of the standard and the unknown (Is+x)

3.4. Catalytic role of the metal oxides

As presented in Fig. 2, the oxidation of the three species in this study takes place in either neutral or acidic media. Hydrochlorothiazide undergoes two dissociation processes with pKa_1= 7.00 and pKa_2 = 9.2 according to the following equilibria; [53]

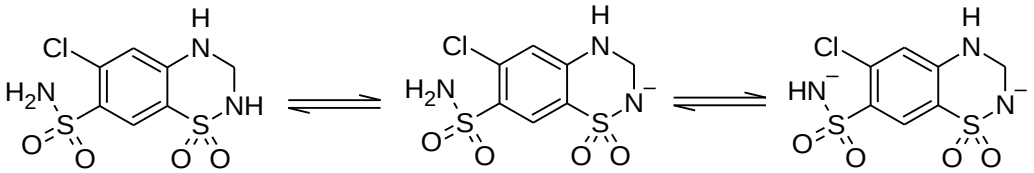

Therefore, at pH =3.00, HCT exists in the most acidic form, the form needed for the oxidation reaction as shown in Fig. 2. As pH increases, the fraction of the acidic species decreases and the probability of HCT oxidation decreases. As mentioned earlier, the utilized pH affects both the structure of the analyzed species as well as the surface structure of the involved catalyst. Pourbaix diagram is the diagram that correlates structure of elements of the periodic table to both the applied voltage and the utilized pH value. According to Pourbaix diagram, at pH 3.00 and potentials close to 1000 mV, manganese exists in the form of manganese dioxide, with Mn(IV) metallic center, which is the catalyst responsible for the HCT oxidation. In this case, manganese oxide acts as both, an oxidizing agent, and a catalyst according to the following equation;

$$C_7H_8ClN_3O_4S_2 + 2MnO_2 \rightarrow C_7H_6ClN_3O_4S_2 + Mn_2O_3 + H_2O$$

The electrons produced from the oxidation of HCT are directly proportional to the amount of HCT exists in proximity to the modified electrode surface. The generated Mn_2O_3 is oxidized back to the Mn (II) oxide under the utilized experimental conditions and the catalytic cycle is repeated again until all of the HCT diffused to the modified surface is consumed. The utilization of manganese dioxide for oxidation of C_1-C_7 organic compounds such as phenol, formaldehyde, and toluene, is common in the literature, usually, manganese is reduced to the 3+ oxidation state and manganese dioxide is converted to Mn_2O_3. [55, 56, 57, 58]

For sulfamethoxazole, pKa_1 = 2.07 and pKa_2 = 7.94, the dissociation processes could be described by the following equilibria; [59]

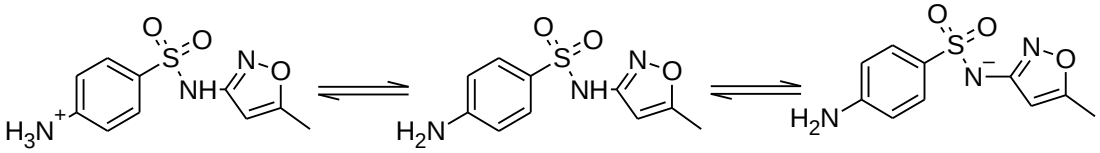

Therefore, it is expected that the major species predominates at pH 7.00 is the neutral form of SMX. According to the Henderson-Hasselbalch equation, the neutral intermediate species exists at the utilized pH is almost nine times the amount of its conjugate base. In addition, the employed pH secures the presence of molybdenum (based on Molybdenum Pourbaix diagram) [60] in the form of a hexavalent ion with a high affinity toward the oxidation of the SMX exists in its neutral form. The oxidation reaction could be described as;

$$MoO_4^{2-} + C_{10}H_{11}N_3O_3S + 2H^+ \rightarrow C_6H_5NO + C_4H_6N_2O + MoO_2 + H_2SO_3$$

The oxidation of TMP could be explained in a similar manner; TMP is a diprotic weak acid with pKa_1 = 3.23 and pKa_2 = 6.76, it dissociates according to;

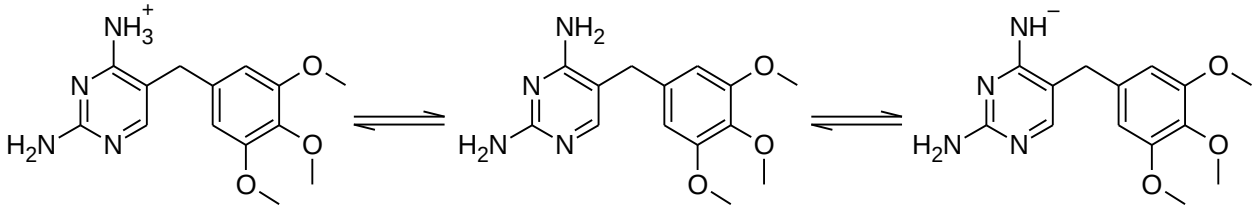

At pH 7.00, the intermediate neutral form is not the predominant species, however, it does exist in a significant amount, almost half that of the most basic form according to the Henderson-Hasselbalch equation. At the molybdenum modified working electrode TMP oxidizes according to the following equation;

$$2MoO_4^{2-} + C_{14}H_{18}N_4O_3 + 4H^+ \rightarrow C_{14}H_{16}N_4O_3 + 2MoO_2 + 3H_2O$$

The produced molybdenum dioxide is oxidized back to the molybdate anion and the oxidation process is repeated again. Role of the molybdate dianion as oxidizing agent has been reported in different studies. The existence of molybdenum ion in the 6+ oxidation state facilitates oxidation reaction of a wide range of organic as well as inorganic species[61,62].

4. CONCLUSIONS

The oxidation of SMX, TMP, and HCT occurs at relatively high potentials, therefore, it must be preceded by the generation of an electron deficient center to facilitate the oxidation step. In this study, MnO_2, and MoO_2, two of the key catalysts used in fuel cells were utilized for the oxidation and as a consequence, detection of three drugs of different pharmaceutical significance. SMX and TMP are antibiotics while HCT is a diuretic. Manganese and molybdenum oxides have electron deficient metallic centers, therefore, they have the potential to oxidize the pharmaceuticals. In addition, the metal oxides enhance the electron transfer rate across the electrode-electrolyte interface, since they are more conductive than bare glassy carbon electrodes.

The proposed catalytic activity was correlated to the utilized pH that tunes structure of the target analyte as well as surface composition of the modified electrodes. Performance of the utilized electrodes could be improved by enhancement of their conductivity and variation of thickness of the acting catalysts, which may be carried out by manipulation of the electro-deposition conditions, such as nature of the electrochemical deposition signal, concentrations of the added modifiers, and pH of the deposition solutions.

ACKNOWLEDGMENTS
The authors would like to thank the School of Graduate Studies at the German Jordanian University for the generous fund needed to finance the conducted work.

References

1. M. Ernst, S. Mann, *Semin. Nephrol*., 31 (2011) 295.
2. D. Seldin, G. Giebisch, Diuretic Agents: Clinical Physiology and Pharmacology, Elsevier, (1997) MA, USA.
3. G. Eknoyan, *Kidney Int. Suppl*., 59 (1997)118.
4. F. Novello, J. Sprague, *J. Am. Chem. Soc.*, 79 (1957) 2028.
5. M. Moser, *Arch. Intern. Med*., 169 (2009) 1851.
6. B. Beermann, M.Groschinsky-Grind, *Eur. J. Clin. Pharmacol*., 12 (1977) 297.
7. R. H. Barbhaiya, W. A. Craig, H. P. Corrick-West, P. G. Welling, *J. Pharm. Sci.*, 71 (1982) 245.
8. R. Nath, M. Saira, *Int. J. Pharm. Pharm. Sci*., 5 (2013) 867.
9. J. A. Mollica, C. R. Rehm, J. B. Smith, H. K. Govan, *J. Pharm. Sci.*, 60 (1971) 1380.
10. H. M. Carapuca, D. J. Cabral, L. S. Rocha, *J. Pharm. Biomed. Anal*., 38 (2005) 364.
11. O. Farghaly, R. Abdel Hameed, H. Abu-Nawwas, *Int. J. Pharm. Sci. Rev. Res.*, 25(2014) 37.
12. M. R. Siddiqui, Z. A. AlOthman, N. Rahman, *Arab. J. Chem*., 10 (2017) S1409.
13. M. E.M. Hassouna, *Anal. Lett*., 30 (1997) 2341.
14. A. U. Kulikov, A. G. Verushkin, L. P. Loginova, *Chromatogrophia*, 61 (2005) 455.
15. A. S. Amin, M. F. EL Shahat, R. E. Edeen., M. A. Meshref, *Anal. Lett*., 41 (2008) 1878.
16. K. B. Alton, D. Desrivieres, J. E. Patrick, *J. Chromatogr. B Biomed. Sci. Appl*., 374 (1986) 103.
17. N. Rawool, A. Venkatchalam, *Indian. J. Pharm. Sci*., 73 (2011) 219.
18. M. I. H. Helaleh, E. S. M. Abu-Nameh, *Chem. Anal-Warsaw*, 43 (1998) 225.
19. M. I. H. Helaleh, E. S. M. Abu-Nameh, R. M. A. Q. Jamhour, *Acta Pol. Pharm*., 55 (1998) 93.
20. M. I. H. Helaleh, E. S. M. Abu-Nameh, *An. Quim*., 94 (1998) 160.

21. M. I. H. Helaleh, T. Korenaga, E. S. M. Abu-Nameh, R. M. A. Q. Jamhour, *Pharm. Acta Helv.*, 73 (1999) 255.
22. A. Shurbaji, M. H. Abu Al Rub, M. M. Saket, E. S. M. Abu-Nameh, *J. AOAC Int*., 93 (2010) 1868.
23. S. A. Nabi, E. S. M. Abu-Nameh, M. I. Helaleh, *J. Pharm. Biomed. Anal*., 17 (1998) 357.
24. O. Abdel Razak, *J. Pharm. Biomed. Anal*., 34 (2004) 433.
25. A. Alghamdi, *J. Food Drug Anal*., 22 (2014) 363.
26. B. Bozal, M. Gumustas, B. Dogan-Topal, B. Uslu, S. A. Ozkan, *J. AOAC Int*., 96 (2013) 42.
27. R. Behzad, S. Damiri, *IEEE Sens. J*., 8 (2008) 1523.
28. C. A. R. Salamanca-NetoPedro, P. H. Hatumura, C. R. T. Talery, E. R. Sartori, Ionics,21 (2014) 1615.
29. H. Beitollahi, F. Ghorbani, *Ionics*, 19 (2013) 1673.
30. M. Gholivand, M. Khodadadian, *Electroanalysis*, 25 (2013) 1263.
31. H. Purushothama, Y. Nayaka, *Sens. Biosensing Res*., 16 (2017) 12.
32. E. Engin, H. Çelikkan, M. L. Aksuc, N. Erka, *Anal. Methods*, 21 (2015) 9254.
33. N. Kumar, R. Goyal, *J. Electrochem. Soc*., 164 (2017) 240.
34. M. C. G. Santos, C. R. T. Tarley, L. H. Dall'Antonia, E. R. Sartori, *Sens. Actuators B Chem*., 188 (2013) 263.
35. W. B. Machini, D. N. David-Parra, M. F. Teixeira, *Eng. Sci. Mater. C*, 57 (2015) 344.
36. C. González-Vargas, N. Serrano, C. Ariño, R. Salazar, M. Esteban, J. M. Díaz-Cruz, *Chemosensors*, 5 (2017) 1.
37. H. Yuqiu, Z. Hongcheng, *Energy Procedia*, 2 (2011) 2769.
38. S. Yan, B. He, *Int. J. Electrochem. Sci*., 12 (2017) 3001.
39. R. Joseph, K. G. Kumar, *Drug Test. Anal*., 2 (2010) 278.
40. I. Cesarino, V. Cesarino, M. R.V. Lanza, *Sens. Actuators B Chem*., 188 (2013) 1293.
41. L. F. Sgobbi, C. A. Razzino, S. A.S. Machado, *Electrochim. Acta*, 191 (2016) 1010.
42. D. L.C. Golinelli, S. A. S. Machado, I. Cesarino, *Electroanalysis*, 29 (2017) 1014.
43. L. S. Andrade, R. C. Rocha-Filho, Q. B. Cass, O. Fatibello-Filho, *Electroanalysis*, 21 (2009)1475.
44. G. N. Calaça, C. A. Pessoa, K. Wohnrath, N. Nagata, *Int. J. Pharm. Pharm. Sci*., 6 (2014) 438.
45. H. D. Herrera-Méndez, P. Roquero, M. A. Smit, L. C. Ordóñez, *Int. J. Electrochem. Sci*., 6 (2011) 4454.
46. O. Marin-Flores, T. Turb, C. Ellefson, K. Wang, J. Breit, J. Ahn, M. G. Norton, S. Ha, *Appl. Catal. B Environ*., 98 (2010) 186.
47. X. Liu, M. Conte, W. Weng, Q. He, R. L. Jenkins, M. Watanabe, D. J. Morgan, D.W. Knight, D. M. Murphy, K. Whiston, C. J. Kiely, G. J. Hutchings, *Catal. Sci. Technol*., 5 (2015) 217.
48. L. C. Ordóñez, P. Roquero, J. Ramírez, P. J. Sebastian, *Int. J. Electrochem. Sci*., 11 (2016) 5364.
49. E. Mehmeti, D. M. Stanković, S. Chaiyo, L. Švorc, K. Kalcher, *Microchim. Acta*, 183 (2016) 1619.
50. Y. Liu, Z. Zhang C. Zhang, W. Huang C. Liang J. Peng, *Bull. Korean Chem. Soc*., 37 (2016) 1173.
51. S. Hameed, A. Munawar, W. S. Khan, A. Mujahid, A. Ihsan, A. Rehman, I. Ahmed, S. Z. Bajwa, *Biosens. Bioelectron*., 89 (2017) 822.
52. C. V. Krishnan, M. Garnett, B. Hsiao, B. Chu, *Int. J. Electrochem. Sci*., 2 (2007) 29.
53. W. Wei, X. Cui, W. Chen, D. G. Ivey, *Chem. Soc. Rev*., 40 (2011) 1697.
54. M. F. Khanfar, N. Al Absi, E. S. M. Abu-Nameh, M. M. Saket, N. Khorma, R. Al Daoud, N. Alnuman, *Int. J. Electrochem. Sci*., 14 (2019) 3265.
55. R. Inguanta, C. Sunseri, Semiconductors: Growth and Characterization, Intech Open, (2018) London, UK.
56. L. Jin , C.-H. Chen, V. M. B. Crisostomo, L. Xu, Y.-C. Son, S. L. Suib, *Appl. Catal. A Gen*., 355 (2009) 169.
57. E. Saputra, S. Muhammad, H. Sun, A. Patel, P. Shukla,Z.H. Zhu, S. Wang, *Catal. Commun*. 26 (2012) 144.

58. H. Lin, D. Chen, H. Liu, X. Zou, T. Chen, *Aerosol Air Qual. Res*., 17 (2017) 1011.
59. P. Feng-Jiao, Y. Guang-Guo, L. You-Sheng, S. Hao-Chang, H. Liang-Ying, *Sci. Total Environ*.
60. A. Davoodi, M. Pakshir, M. Babaiee , G. R. Ebrahimi, *Corros. Sci*., 53 (2011) 399.
61. K. Grudpan, N. Worakijcharoenchai, P. Sooksamiti, J. Jakmunee, G. D. Christian, *Indian J. Chem. Sec. A*, 42A (2003) 2939.
62. S. Zein El Abedin, *J. Appl. Electrochem*., 31 (2001) 711.